

Reversible mechanics and time's arrow

William G. Hoover

*Department of Applied Science, University of California at Davis-Livermore, Livermore, California 94550
and Department of Physics, Lawrence Livermore National Laboratory, Livermore, California 94550*

(Received 4 May 1987; revised manuscript received 6 July 1987)

The microscopic mechanics discovered by Nosé, of which Gauss's isokinetic mechanics is a special case, makes it possible to simulate macroscopic irreversible nonequilibrium flows with purely reversible equations of motion. The Gauss-Nosé and Nosé-Hoover equations of motion explicitly include time-reversible momentum and energy reservoirs. Computer simulations of nonequilibrium steady-state systems described by Gauss-Nosé mechanics invariably evolve in such a way as to increase entropy. The corresponding phase-space distribution functions, which include reservoir degrees of freedom, collapse onto stable strange attractors. Hypothetical time-reversed motions, which would violate the second law of thermodynamics, cannot be observed for two reasons: First, such reversed motions would occupy zero volume in the phase space; second, they would be dynamically unstable. Thus, Nosé's reversible mechanics is fully consistent with irreversible thermodynamics, in the way forecast by Prigogine. That is, the consistency follows from the formulation of new microscopic equations of motion.

I. INTRODUCTION

Over 100 years ago Boltzmann derived his H Theorem. The theorem describes a reasonable microscopic basis for the macroscopic second law of thermodynamics. Because Boltzmann's derivation was approximate—he replaced the actual reversible equations of motion with an irreversible approximation—Boltzmann's work was criticized, and on two slightly different grounds.

First, any system evolving in time according to time-reversible equations of motion can be propagated backward. Time reversibility implies that any trajectory along which entropy increases corresponds to a time-reversed trajectory along which entropy decreases. This first objection to the H theorem is Loschmidt's reversibility paradox.

Second, for a finite phase space, Hamilton's microscopic motion equations imply that a trajectory will eventually return to the neighborhood of its initial state. This implies again that any trajectory containing an entropy increase must also contain, equally often, a corresponding entropy decrease. This second objection to the H Theorem is the Poincaré-Zermélo recurrence paradox.

A convincing explanation of the irreversibility inherent in the exact equations of motion, without making Boltzmann's approximation, had to await fast computers. These machines make it possible to study the nonlinear systems with the three-or-more-dimensional "state spaces"—the generalized phase spaces including thermodynamic boundary variables—required for chaotic behavior. Prigogine has steadfastly maintained that a proper understanding of irreversibility requires new microscopic equations, beyond Newton's and Schrödinger's. For a popular account see the February 1987 issue of *Discover* magazine.¹ The validity of Prigogine's view is confirmed, in what follows, by relat-

ing the second-law irreversibility of microscopically reversible macroscopic systems to the properties of a new mechanics recently discovered by Nosé.²⁻⁴

With the advent of computers irreversibility could be studied numerically. The first studies examined the approach to equilibrium of isolated systems. At Los Alamos, Fermi, Pasta, and Ulam found striking evidence that microscopically reversible systems never reach equilibrium, but instead exhibit Poincaré-Zermélo recurrence relatively quickly.⁵ On the other hand, at Livermore, Wainwright and Alder found quantitative agreement between their hard-sphere entropy evolution and the predictions of Boltzmann's equation, on which the H -theorem irreversibility proof is based.⁶

By 1972 extensive studies involving systems driven away from equilibrium were underway. It became feasible to examine many-body viscous flows and heat flows by direct simulation,⁷ using reversible equations of motion to describe not only the Newtonian system which is traversed by the nonequilibrium momentum and energy fluxes, but also the non-Newtonian reservoir regions which drive these fluxes. It was not until about ten years later, when Evans and I explored the structure of the underlying differential motion equations, that Ashurst's work on isokinetic dynamics was recognized as a time-reversible application of Gauss's 160-year-old "Principle of Least Constraint"⁸

$$\sum (F_c)^2 / (2m) \text{ minimum} . \quad (1)$$

This principle (1) states that *any* constraint, including those imposed by Ashurst on his isokinetic reservoirs, should be imposed with the smallest possible constraint forces F_c , in the least-squares sense of the principle (1).

II. NOSÉ AND NOSÉ-HOOVER MECHANICS

(REFS. 2-4)

Just a few years ago Nosé posed an interesting question: Which microscopic dynamical equations of motion are consistent with Gibbs's macroscopic equilibrium ensembles, such as the canonical and isothermal-isobaric ensembles? Nosé found the answer in terms of new time-reversible Hamiltonian equations of motion. This approach required a "time-scaling variable" s and a corresponding set of scaled momenta $\{p/s\}$.

In an equivalent approach now called "Nosé-Hoover" mechanics, I emphasized⁹ that the time-scaling is not only cumbersome, but also unnecessary. In Nosé-Hoover mechanics the usual Hamiltonian equation of motion, $\dot{p}=F$, is replaced with a generalized friction-coefficient form:

$$\dot{p}=F-\zeta p, \quad (2)$$

where the deterministic and reversible friction coefficient ζ itself obeys a first-order evolution equation:

$$\dot{\zeta}=[(K/K_0)-1]/\tau^2. \quad (3)$$

At equilibrium, ζ has a Gaussian distribution centered on zero.⁹ K is the kinetic energy, which fluctuates around the value K_0 , and τ is a relaxation time for the reservoir which maintains the canonical temperature $2K_0/(3Nk)$. In an equilibrium N -body system, the fluctuations in ζ are of order $(1/N)^{1/2}$ so that the Nosé-Hoover equations of motion converge to the Newtonian ones in the thermodynamic limit. In the Gauss-Nosé isokinetic limit,⁷ where the reservoir relaxation time τ approaches zero, the kinetic energy is a constant of the motion. In the approach to this isokinetic limit the Nosé-Hoover coordinate and momentum deviations from their limiting values vanish as τ^2 and τ , respectively.¹⁰ The limiting Gauss-Nosé trajectories are reproduced by the explicit friction coefficient

$$\zeta=-\dot{\Phi}/(2K_0), \quad (4)$$

where $\dot{\Phi}$ is the time rate of change of the potential energy.

Though they are *not Hamiltonian* the Nosé-Hoover equations, (2) and (3), and the Gauss-Nosé equations, (2) and (4), are *time reversible*, where the quality of time reversibility implies that a movie showing any solution of the equations, when run backward through a projector, shows a (reversed) reversible solution satisfying the *same* equations of motion. The reversibility can be understood physically by following Nosé's derivation,^{2,3} in which the equilibrium canonical-ensemble friction coefficient ζ arises as the momentum conjugate to the time-scaling variable s . We illustrate the difference between the Nosé and Nosé-Hoover equations of motion for a simple one-body example problem in Sec. IV. The Nosé-Hoover non-Hamiltonian equations of motion are *much* more useful than the original Hamiltonian ones because they suggest ways to relate not only Gibbs's statistical thermodynamics, but also the nonequilibrium fluid and solid mechanics of Navier and Stokes, directly

to atomistic reversible molecular dynamics. In the nonequilibrium generalization of Nosé's work, different reservoir regions obeying Nosé mechanics can be connected to Newtonian regions,^{3,11,12} as indicated in Fig. 1. *Many* reservoirs can be used, not necessarily just two, or particular degrees of freedom can be maintained at different temperatures in order to study vibrational relaxation.¹¹

It has to be emphasized that the Gauss-Nosé, Nosé, and Nosé-Hoover equations of motion differ in a fundamental way from irreversible equations of motion such as the Langevin equation. The time reversibility is essential to understanding the topological nature of nonequilibrium phase-space distributions and to resolving the paradox that microscopic reversibility underlies macroscopic irreversibility. The study of macroscopic irreversibility from reversible equations of motion has intensified during the last four years, with an emphasis on finding the simplest possible systems maintaining both reversibility and thermodynamic significance. The shear viscosity of a two-body system,¹³ the heat conductivity of a three-body system,¹⁴ and the mobility of a two-body system¹⁵ were all studied using the Gauss-Nosé equations of motion.

III. FRACTAL ATTRACTORS, LYAPUNOV EXPONENTS, AND DIMENSIONALITY LOSS

The mobility study,¹⁵ equivalent to following the field-driven constant-speed motion of a point mass through a "Galton board," that is, through a regular two-dimensional triangular lattice of hard-disk elastic scatterers, produced clear direct evidence for fractal objects, "strange attractors," from *time-reversible* equations of motion. Such attractors are usually associated with qualitatively different dissipative time-irreversible equations or with (time-irreversible) maps. The Galton-board phase-space attractor sections, and subsequent similar Poincaré sections describing field-driven diffusion in a sinusoidal "Frenkel-Kontorova" potential,¹⁶ were amazing. Rather than revealing distribution functions amenable to Fourier or Tschebyshev expansion, these simple nonequilibrium problems instead generated fractal objects, such as those shown in Fig. 2. Fractal objects such as these characteristically show a discontinuous structure at arbitrarily small scales of observation.¹⁷ The reasonable idea of expanding nonequilibrium distribution functions as sums of orthogonal functions cannot work

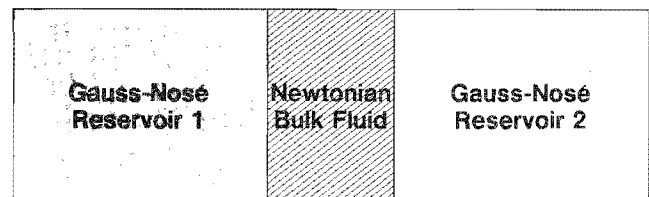


FIG. 1. A steady-state time-reversible nonequilibrium system in which two reservoirs, with Gauss-Nosé or Nosé-Hoover mechanics applied to at least some degrees of freedom, are linked to a bulk Newtonian nonequilibrium region.

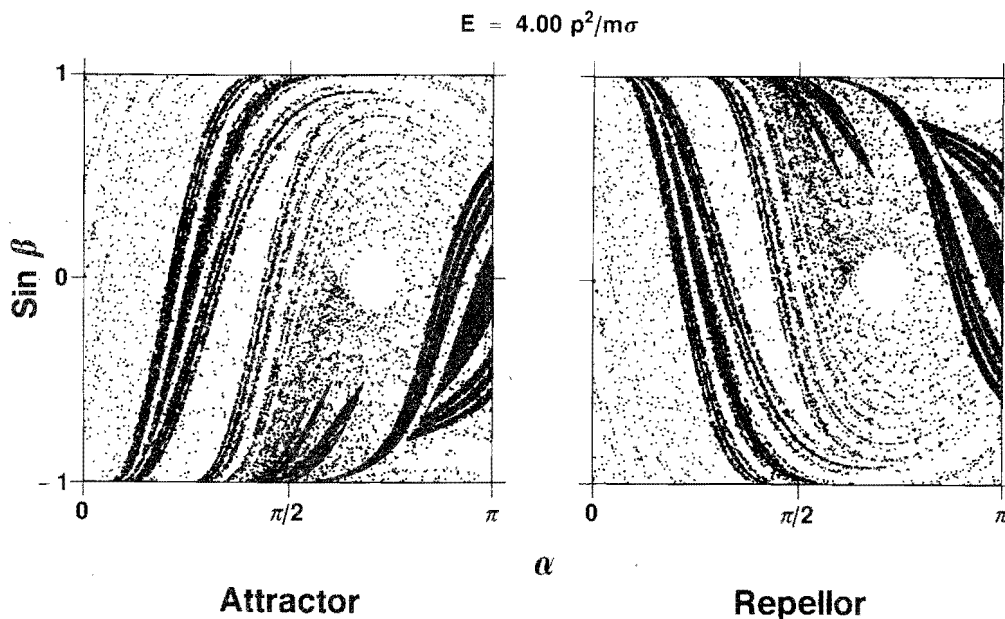


FIG. 2. Section of a typical fractal object representing a small-system nonequilibrium simulation. The problem (a mass point falling at constant kinetic energy in a two-dimensional "Galton board") is discussed in Ref. 15. The field driving the motion of the scattering point is E and the scatterers are arranged in a triangular lattice. The angle α measures the point of collision relative to the field direction. The angle β gives the direction of the scattering point's velocity after a (hard-disk) collision, relative to the radial vector linking the interacting particles.

for such problems, even in the linear region described by the Green-Kubo theory.

To begin a quantitative characterization of these reversible dissipative systems it is useful to follow Benettin's lead¹⁸ by determining the spectrum of Lyapunov exponents $\{\lambda_i\}$. This can be done for both equilibrium systems and far-from-equilibrium Nosé-Hoover systems. The Lyapunov exponents describe the exponential growth and decay rates of objects in phase space. The one-dimensional distance between two neighboring points which move following the equations of motion increases as the exponential of $(\lambda_1 t)$, the two-dimensional area defined by three moving trajectory points increases as the exponential of $(\lambda_1 t + \lambda_2 t)$, the four-point three-dimensional volume increases as the exponential of $(\lambda_1 t + \lambda_2 t + \lambda_3 t)$, and so on. The reversibility of the equations determining these exponents shows that, for steady flows, the reversed trajectories have reversed Lyapunov spectra, with each λ_i in the forward direction becoming $-\lambda_i$ in the backward reversed direction. This important symmetry property would be successfully disguised were we to use stochastic motion equations, such as the Langevin equation, rather than Nosé's. The spectra, for dense fluids such as a Lennard-Jones fluid, turned out to have approximately a Debye form,^{19,20} as shown in Fig. 3, with a maximum Lyapunov exponent equal to a typical atomic vibration frequency.

The time reversibility of the Lyapunov spectrum implies just two possibilities: a phase-space hypervolume centered on a comoving trajectory can either move with a constant hypervolume, with equal numbers of positive

and negative Lyapunov exponents, or can alternatively grow in one time direction and shrink in the other direction of time. This latter possibility is an "Arrow of Time,"²¹ and has in fact been observed in every single nonequilibrium Gauss-Nosé or Nosé-Hoover simulation studied so far, including Morriss's recent study of two-body shear flow.²¹ It is physically apparent, for a steady dynamical state, that the full phase-space hypervolume cannot be an increasing function of time. In every case, in the forward direction of time the phase-space hypervolumes shrink to a stable fractal object. This fractal at-

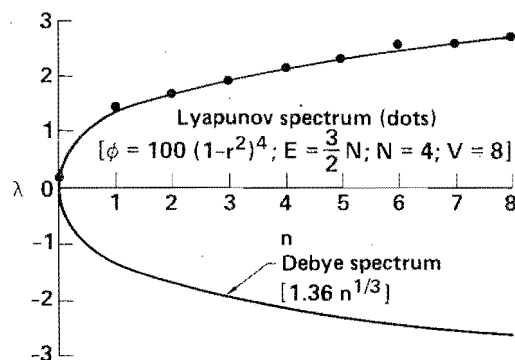


FIG. 3. A typical dense-fluid Lyapunov spectrum, showing the resemblance to the cube-root Debye spectrum drawn as a smooth curve. Nine of the 18 Lyapunov exponents are shown. The system is a four-body three-dimensional dense fluid with a short-ranged repulsive potential cut off at the value $r=1$ and with an anharmonicity resembling that of the Lennard-Jones potential.

tractor is stable in the sense that its volume is continuously shrinking, and reaches a steady-state limit of zero. The reversed "repellor" state—just like the attractor but with the signs of all the momenta and friction coefficients reversed—is unstable. The corresponding repeller Lyapunov spectrum has a positive sum, corresponding to phase-space growth and instability. Sections of a simple attractor-repellor pair are shown in Fig. 2.

Thus the situation is this. Nonequilibrium systems very quickly (in a physical time of order picoseconds) collapse onto a stable fractal subspace of the complete equilibrium phase space. The logarithmic rate at which the volume decreases is exactly the rate at which entropy, divided by Boltzmann's constant, is generated. Within the zero-volume fractal subspace the incredible churning motion described by the attractor is chaotic and formally reversible. But, the time-reversed trajectory is actually unstable, with predominantly positive Lyapunov exponents. The zero phase-space volume of the corresponding repeller (reversed attractor) coupled with its evolutionary instability, guarantees that (1) the repeller cannot be located, and that (2) any approximate effort to locate and follow a reversed trajectory will soon fail. The only effective way to find a repeller (which would violate the second law of thermodynamics) is to run a known attractor trajectory backward in time.

An interesting feature common to all the Gauss-Nosé and Nosé-Hoover calculations is the effective loss of degrees of freedom inherent in the lowered fractal dimensionality of the phase-space attractors. Figure 1 shows a typical situation, in which a bulk Newtonian system is driven away from equilibrium by two adjacent reservoir regions. In a real system, this loss must occur in the nonequilibrium Newtonian region, shown in the center of the figure, rather than in the driving reservoir regions shown adjacent to the bulk region. It is clear, from the relatively small dependence of transport coefficients on system size, that the thermostatted boundaries have little effect on the phase-space dimensionality loss ΔD .²² Thus the fractal phase-space structure characterizes not the boundaries, but rather the bulk Newtonian part of the system. A many-body example is discussed in Sec. V. The bulk system's dimensionality loss is extensive, and depends only on the magnitude of the departure from equilibrium.

To estimate the dimensionality loss ΔD we simply ask for the *maximum* dimensionality, D_{\max} , of a phase-space object which still *increases* its hypervolume with time. For the subspace volume to increase, the sum of the D_{\max} largest Lyapunov exponents, $\lambda_1 + \lambda_2 + \dots + \lambda_{D_{\max}}$, must be positive, but so close to zero that adding one more term makes the sum negative. If the system is not too far from equilibrium then the remaining (negative) Lyapunov exponents are all close to the minimum value, $-\lambda_1 = \lambda_N = -\nu$, where ν is a frequency of order the Debye frequency. Thus the dimensionality loss is approximately

$$\Delta D = \dot{S} / (k\nu), \quad (5)$$

where \dot{S} is the rate of irreversible entropy production

and k is Boltzmann's constant. For water, sheared at a strain rate of 10^5 Hz, the loss of degrees of freedom is about one billion per cubic centimeter, independent of the number of degrees of freedom used in the thermo- stats which drive the motion.

IV. ONE-BODY ONE-RESERVOIR ONE-DIMENSIONAL EXAMPLE (REF. 20)

To make the connection between irreversibility, fractals, and Lyapunov spectra clearer, it is useful to consider examples. The simplest example is that of a one-dimensional particle, accelerated by a field but maintained at constant temperature by Nosé or Nosé-Hoover equations of motion. The example is interesting too in pointing out the qualitative differences between these two closely related approaches. To avoid complexity we set the temperature T , Boltzmann's constant k , the relaxation time τ , particle mass m , and field strength g all equal to unity. Nosé's Hamiltonian for this situation is

$$H_{\text{Nosé}} = [p_x^2 / (2s^2)] + (p_s^2 / 2) - x + \ln s. \quad (6)$$

The equations of motion

$$\begin{aligned} \dot{x} &= [p_x / (s^2)], \quad \dot{p}_x = 1, \quad \dot{s} = p_s, \\ \dot{p}_s &= [(p_x / s)^2 - 1] / s \end{aligned} \quad (7)$$

have the solution

$$x = \ln t, \quad p_x = t, \quad s = t, \quad p_s = 1, \quad (8)$$

so that *this* Hamiltonian system has *no* steady-state behavior at long times. On the other hand, Nosé's *scaled* equations of motion, with each of the rates in (7) multiplied by the scaling factor s , are

$$\dot{x} = (p_x / s), \quad \dot{p}_x = s, \quad \dot{s} = s p_s, \quad \dot{p}_s = [(p_x / s)^2 - 1], \quad (9)$$

with the solution

$$x = t, \quad p_x = e^t, \quad s = e^t, \quad p_s = 1. \quad (10)$$

where the "new" time, t in (10), is the *logarithm* of the "old" time, t in (8). Finally, the Nosé-Hoover equations for this same problem, equivalent to (9), but with p replacing p_x / s and ζ replacing p_s , are

$$\dot{x} = p, \quad \dot{p} = 1 - \zeta p, \quad \dot{\zeta} = p^2 - 1, \quad (11)$$

which have the (stable) solution

$$x = t, \quad p = 1, \quad \zeta = 1 \quad (12)$$

[where t in (12) and t in (10) coincide] corresponding to *steady* motion with the potential energy gained from the field being extracted by the friction coefficient ζ .

This example is a particularly interesting one because it illustrates the way in which the *same* trajectory (in $x p_x s p_s$ space) can correspond, when traversed at different nonuniform rates, to very different physical behaviors. In the "scaled-time" picture (10) or the Nosé-Hoover picture (12) a well-defined steady state with a nonzero current results. In the original Nosé Hamiltonian picture (8) a transient state results instead. The rela-

relationship between the two solutions is interesting. Because the relationship between the "new" scaled time in (10) and (12) and the "old" Hamiltonian time in (8) is logarithmic, the interval of "old" time required to see a fixed interval of "new" steady-state time increases exponentially fast. Thus the nonequilibrium scaled-time solution or the equivalent Nosé-Hoover solution give a steady state which is simply not observable in Nosé's original Hamiltonian picture.

V. EIGHT-BODY TWO-RESERVOIR THREE-DIMENSIONAL EXAMPLE

Consider a dense three-dimensional periodic fluid of particles interacting with the purely repulsive potential

$$\phi = 100(1-r^2)^4 \quad (r < 1). \quad (13)$$

For convenience we choose the particle mass, diameter, specific volume V/N , and Boltzmann's constant all equal to 1. If we choose one particle to be "hot," with temperature T_h , and another to be "cold," with temperature T_c , we expect to see a flow of heat from the hot particle to the cold particle, with the remaining six particles taking up an intermediate temperature. To fix the center of mass of the system we use the equations of motion

$$\dot{p}_i = F_i - \xi_i p_i + \langle \zeta p \rangle, \quad i = h \text{ or } c \quad (14)$$

for the reservoir particles, where $\langle \zeta p \rangle$ is the *instantaneous* average, $(\zeta_h p_h + \zeta_c p_c)/8$. The phase space describing this system, with the center of mass fixed, is $6(N-1)+2=44$ dimensional. For the six Newtonian particles the equation of motion is

$$\dot{p}_j = F_j + \langle \zeta p \rangle, \quad j = 3-8. \quad (15)$$

Numerical work, using Nosé-Hoover thermostats, shows that such a system is stable and well behaved.

As an illustration we choose the special case with the two temperatures equal to 1.0 and 0.1, with the friction coefficients determined by the equations $\xi_i = p^2 - 3T_i$. Average potential and kinetic energies of 2.5 and 8 result. The steady-state values of the hot and cold friction coefficients are, respectively -1.6 and $+16$. This corresponds to an *energy* transfer rate of $3 \times 1.6 = 0.3 \times 16$ and an entropy loss rate $-3 \times (1.6 - 16) \times (\frac{7}{8}) = 38$, where the factor of $\frac{7}{8}$ results from the center-of-mass term in the equations of motion. The thermodynamic state is close to one for which the entire equilibrium Lyapunov spectrum is known.²⁰

Now what are the implications of these observations in terms of the fractal phase-space attractors discussed in Sec. III? The steady energy balance between the power furnished to the hot particle and that absorbed by the cold particle corresponds to an entropy loss rate of 38. Because the Lyapunov spectra are insensitive to departures from equilibrium we expect that the 14 most negative of the 44 exponents vary roughly linearly between -3.5 and -2.5 , so that a larger entropy loss rate, at least $14 \times 3 = 42$, would be required to reduce the occupied nonequilibrium phase-space attractor dimensionality by 14. Thus hot and cold temperatures of 1.0

and 0.1 are not sufficiently different to reduce the phase-space dimensionality below the bulk value. The number of degrees of freedom which must be added, in reservoirs, to maintain a nonequilibrium steady state, usually exceeds the dimensionality loss of the combined reservoir + bulk + reservoir phase space.

But it has to be emphasized that the reservoirs generally play no role in the loss of dimensionality. A "hot" reservoir typically *gains* entropy (phase-space volume) from the action of the frictional forces required to maintain its temperature. It simultaneously *loses* an exactly equivalent entropy through heat flow to its neighboring Newtonian system. Likewise, the frictional and Newtonian heat transfers cancel for a "cold" reservoir. *Only* in the Newtonian region, which alone is far from equilibrium, is the phase space contracted. It is clear that reservoir regions so different in condition as to drive a system into a periodically repeating "limit cycle" can actually reduce the total number of degrees of freedom required to describe the phase space to unity, corresponding to the time measured along the periodic solution.

VI. THREE-BODY TWO-RESERVOIR TWO-DIMENSIONAL EXAMPLE

In order to study the simplest example incorporating realistic Newtonian dissipation in conjunction with hot and cold reservoirs, consider a two-dimensional three-body system modeled after Fig. 1. The height is 2 and the width $1 + 1 + 1 = 3$. The short-range repulsive interaction potential is given by (13). Thus a single Newtonian particle transmits heat between hot and cold Nosé-Hoover reservoir particles. Lyapunov spectra were determined for a variety of temperature differences, not just in the complete 14-dimensional phase space, but also in the two five-dimensional reservoir phase spaces and the four-dimensional Newtonian phase space. The spectra were determined by following the motion of basis vectors (14 in the full space, 5 or 4 in the subspaces) constrained to remain orthonormal as explained in Ref. 19.

The time-averaged histories of these basis vectors provide a detailed account of the dynamical instability and dissipation present in a system far from equilibrium. But it is not a simple matter to apportion the dissipation and irreversibility among the three interacting particles or among their corresponding subspaces. The Lyapunov spectrum for a Newtonian subspace necessarily sums to zero. The Lyapunov spectra for the cold and hot subspaces have sums which are respectively negative and positive. And a *positive* Lyapunov sum has no meaningful geometrical interpretation in a steady state.

The projections of the orthonormal basis vectors are also hard to interpret, although this situation may improve as more experience with a variety of problems becomes available. The basis vectors with the *largest* rms projections in the friction-coefficient directions typically correspond to small Lyapunov exponents near zero. The basis vector associated with the most negative Lyapunov exponent had substantial projections onto the subspaces of all three particles, but with the greatest components corresponding to the highest-temperature particle. Like-

wise the basis vector associated with the most positive Lyapunov exponent had its greatest projections in the hot-particle subspace. A more-detailed localization and identification of the microscopic site of second-law irreversibility is the tantalizing goal of ongoing studies of basis-vector dynamics.²³

VII. SUMMARY AND CONCLUSION

To summarize the situation, about 40 years after Fermi's pioneering work at Los Alamos, fast computers have been used to show that the macroscopic second law of thermodynamics is a natural consequence of reversible microscopic equations of motion. Further, the paradoxical reversed states, which could theoretically violate the second law, are not only invisible (because they occupy a zero-phase-space-volume repeller) but also unstable. The recurrence paradox does not apply to steady states such as those generated using Nosé's mechanics. Such states obey the second law of thermodynamics on both short and long time scales. It is both natural and physically reasonable that dissipative steady states do nearly recur repeatedly, as time goes on.

The simplicity and utility of Nosé's idea of using feedback to link thermodynamics to mechanics suggest promising applications in fluid and solid mechanics and in plasma physics, particularly in problems where boundary interactions currently frustrate numerical

work. The structure of Nosé's equations lies a little outside the traditional range of mathematicians in that these equations have no fixed points.²⁴ For this reason, the topology of Nosé trajectories, and the strange attractors associated with steady-state trajectories, deserve further investigation. The main problem still remaining is to understand the analogous situation in quantum physics. Preliminary investigations suggest that Nosé's Hamiltonians will play a key role in resolving this question. It is interesting to note that the simplest such problem, a Nosé particle in a periodic one-dimensional box, is exactly equivalent to the two-dimensional hydrogen atom studied by Asturias and Aragón.²⁵

ACKNOWLEDGMENTS

I thank many individuals for their help in this investigation of irreversibility: Bill Ashurst, Giovanni Ciccotti, Denis Evans, Daan Frenkel, Mike Gillan, Lew Glenn, Brad Holian, Tony Ladd, Bill Moran, Carl Moser, Shūichi Nosé, Harald Posch, Ed Saibel, Wilson Talley, Tom Wainwright, and Fred Wooten. This work was supported by the United States Army Research Office, at the University of California at Davis. Work at Livermore was performed under the auspices of the United States Department of Energy under University of California Contract No. W-7405-ENG-48.

¹T. Rothman, *Discover* **8**(2), 62 (1987); **8**(5), 100 (1987).

²S. Nosé, *J. Chem. Phys.* **81**, 511 (1984); *Mol. Phys.* **52**, 255 (1984).

³S. Nosé, *Mol. Phys.* **57**, 187 (1986).

⁴W. G. Hoover, *Molecular Dynamics*, Vol. 258 of *Lecture Notes in Physics* (Springer-Verlag, Heidelberg, 1986).

⁵E. Fermi, J. Pasta, and S. Ulam, Los Alamos Scientific Laboratory Report No. LA-1940, 1955 (unpublished), reprinted in *Stanislaw Ulam, Sets, Numbers, and Universes: Selected Works*, edited by W. A. Beyer, J. Mycielski, and G.-C. Rota (M.I.T. Press, Cambridge, MA, 1974), pp. 491–501. See also J. L. Tuck and M. T. Menzel, *Adv. Math.* **9**, 399 (1972).

⁶B. J. Alder and T. E. Wainwright, *Proceedings of I.U.P.A.P. Symposium on Transport Processes in Statistical Mechanics, Brussels, 1956*, edited by I. Prigogine (Interscience, New York, 1958), p. 97.

⁷W. T. Ashurst, Ph. D. dissertation, University of California at Davis–Livermore, 1974.

⁸L. A. Pars, *A Treatise on Analytical Dynamics* (Oxbridge, Woodbridge, CT, 1979); D. J. Evans, W. G. Hoover, B. H. Failor, B. Moran, and A. J. C. Ladd, *Phys. Rev. A* **28**, 1016 (1983).

⁹W. G. Hoover, *Phys. Rev. A* **31**, 1695 (1985).

¹⁰B. L. Holian and W. G. Hoover (unpublished).

¹¹B. L. Holian, in *Molecular Dynamics Simulation of Statistical-Mechanical Systems*, Proceedings of the International School of Physics "Enrico Fermi," Course XCVII, Varenna, 1985, edited by W. G. Hoover and G. P. F. Ciccotti, (North-Holland, Amsterdam, 1986); B. L. Holian, *J. Chem. Phys.* **84**, 3138 (1986).

¹²B. L. Holian, W. G. Hoover, and H. A. Posch, *Phys. Rev. Lett.* **59**, 10 (1987); W. G. Hoover, B. Moran, B. L. Holian, H. A. Posch, and S. Bestiale, in *Computer Simulation of*

Nonequilibrium Processes, Proceedings of the Fifth Topical Conference on Shock Waves in Condensed Matter, Monterey, California, 1987, edited by N. C. Holmes and S. C. Schmidt (North-Holland, Amsterdam, in press).

¹³A. J. C. Ladd and W. G. Hoover, *J. Stat. Phys.* **38**, 973 (1985); G. P. Morriss, *Phys. Lett.* **113A**, 269 (1985).

¹⁴W. G. Hoover and K. W. Kratky, *J. Stat. Phys.* **42**, 1103 (1986).

¹⁵B. Moran, W. G. Hoover, and S. Bestiale, *J. Stat. Phys.* **48**, 709 (1987).

¹⁶W. G. Hoover, H. A. Posch, B. L. Holian, M. J. Gillan, M. Mareschal, C. Massobrio, and S. Bestiale, *Mol. Simulation* (to be published).

¹⁷B. B. Mandelbrot, *Fractal Geometry of Nature* (Freeman, San Francisco, 1982).

¹⁸G. Benettin, L. Galgani, and J. Strelcyn, *Phys. Rev. A* **14**, 2338 (1976).

¹⁹W. G. Hoover and H. A. Posch, *Phys. Lett.* **113A**, 82 (1985); **123A**, 227 (1987); for equilibrium and nonequilibrium 32-particle examples see H. A. Posch and W. G. Hoover, *Chaotic Dynamics in Dense Fluids*, in *Proceedings of the European Physical Society, 1987*, Vol. 11G, p. 17.

²⁰W. G. Hoover, H. A. Posch, and S. Bestiale, *J. Chem. Phys.* (to be published).

²¹G. P. Morriss, *Phys. Lett.* **122A**, 236 (1987).

²²D. J. Evans and B. L. Holian, *J. Chem. Phys.* **83**, 4069 (1985).

²³W. G. Hoover, B. L. Holian, and H. A. Posch (unpublished).

²⁴R. S. Westfall, *Never at Rest: a Biography of Isaac Newton* (Cambridge University Press, Cambridge, England, 1981).

²⁵F. J. Asturias and S. R. Aragón, *Am. J. Phys.* **53**, 893 (1985).